ISSN 1070-4272, Russian Journal of Applied Chemistry, 2017, Vol. 90, No. 1, pp. 91−96. © Pleiades Publishing, Ltd., 2017.
Original Russian Text © S.S. Tulenin, A.A. Timina, L.N. Maskaeva, V.F. Markov, 2017, published in Zhurnal Prikladnoi Khimii, 2017, Vol. 90, No. 1, pp. 98−103.

VARIOUS TECHNOLOGICAL PROCESSES

Chemical Bath Deposition of Thin Nanocrystalline Tin(II) Sulfide Films with Thioacetamide

S. S. Tulenin[a], A. A. Timina[a], L. N. Maskaeva[a,b]*, and V. F. Markov[a,b]

[a] *Ural Federal University after name the First President of Russia B.N. Yeltsin, ul. Mira 19, Yekaterinburg, 620002 Russia*
[b] *Ural Institute of State Firefighting Service, Ministry of Emergency Situations of the Russian Federation, ul. Mira 22, Yekaterinburg, 620137 Russia*
**e-mail: mln@ural.ru*

Received November 30, 2016

Abstract—Nanocrystalline tin(II) sulfide layers 100–650 nm thick were prepared by hydrochemical deposition on glass–ceramic supports from a citrate system at 323−343 K using thioacetamide as chalcogenizing agent. These films are of interest for the development of thin-film solar radiation converters based on the multicomponent compound Cu_2ZnSnS_4 of kesterite structure, prepared using a cost-saving process. Examination by scanning electron microscopy shows that tin(II) sulfide layers are formed from spherical nanocrystallites of 20–40 nm size. X-ray diffraction analysis shows that they crystallize in the orthorhombic system with the unit cell parameters a = 4.276, b = 11.243, and c = 3.986 Å. Analysis by X-ray photoelectron spectroscopy revealed the presence of up to 44.86 at. % oxygen in the surface layer of the film. This oxygen is mainly present in surface contaminants and is also incorporated in SnO present on the surface.

DOI: 10.1134/S1070427217010141

Compounds based on tin(II) sulfide substitude today a particular place among materials sensitive in the visible and near-IR range [1]. They are widely used as a base of the multicomponent compound Cu_2ZnSnS_4 of kesterite structure, from which thin-film solar energy converters are prepared [2−5], and also as photoconductors, semiconductor sensors, and microcells used in robotic engineering, medicine, and space and military engineering [6, 7].

The majority of the existing methods for preparing tin(II) sulfide in the form of thin films are based, as a rule, on physical procedures and have a number of disadvantages such as the use of high temperatures, high vacuum, and sophisticated equipment [1, 2, 8]. On the other hand, the procedure for hydrochemical deposition of SnS from aqueous solution is of much interest [9–11]. The method is simple and power-saving and allows wide variation of the composition and functional properties of the materials by using different complexing and sulfudizing agents. However, the main problem in hydrochemical synthesis of SnS films is the choice of the formulation and determination of the optimum deposition conditions.

A number of published papers deal with thin tin sulfide films prepared from alkaline solutions using thiourea CSN_2H_4 as chalcogenizing agent [11−13]. The thermodynamic calculations of the conditions for the formation of the SnS phase are performed, and the composition of the deposition baths is suggested. Sodium thiosulfate [14, 15] and ammonium sulfide [16] are also used as chalcogenizing agents for the synthesis of tin sulfide films. The layers synthesized in these studies are relatively thick (up to 400–500 nm), but have heterogeneous composition and imperfect crystal structure. Such papers are scarce and, as a rule, consist in search for the deposition conditions. In the majority of studies, tin sulfide films were deposited from weakly acidic solutions using thioacetamide $CSCH_3NH_2$ [17−20]. It should be noted that many researches focus their attention on formulations without studying in detail the nucleation and growth of the solid phase, which also exert a decisive effect on the structure and properties of

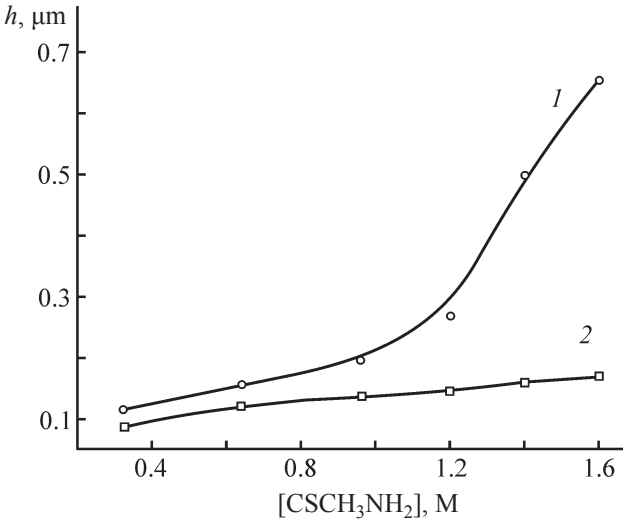

Fig. 1. Thickness h of SnS films prepared by chemical deposition from (*1*) tartrate and (*2*) citrate–tartrate mixtures as a function of the $CSCH_3NH_2$ concentration.

the films. Furthermore, the synthesis process in some of these studies is not examined comprehensively, and the influence exerted by the reaction mixture composition and support material on the microstructure and molecular design of the films is not discussed.

In this work, we prepared tin(II) sulfide films by hydrochemical deposition using thioacetamide as chalcogenizing agent and studied the structure, composition, and morphology of the layers obtained in relation to the synthesis conditions.

EXPERIMENTAL

Hydrochemical synthesis of tin sulfide films was performed for comparison from two systems: tartrate and citrate–tartrate. The tartrate bath contained $SnCl_2$ (pure grade), aqueous solution of tartaric acid $C_4H_6O_6$ (analytically pure grade), and thioacetamide $CSCH_3NH_2$ (chemically pure grade); the citrate–tartrate mixture contained, along with the above compounds, also sodium citrate $Na_3C_6H_5O_7$ (analytically pure grade) for additional binding of Sn^{2+} ions.

Tin sulfide films were deposited onto preliminarily degreased glass–ceramic supports in the temperature interval 323−343 K in sealed reactors made of molybdenum glass. The reactors were placed in an LOIP LT-100 thermostat with which the temperature can be maintained with an accuracy of ±0.1°C. The film deposition time was from 40 to 120 min.

The thickness of the synthesized SnS layers was evaluated with an MII-4 interference microscope (Linnik microinterferometer).

The film morphology was studied by scanning electron microscopy with a Mira-3-LMY device. The electron beam accelerating voltage was 10 kV.

The composition and main forms of chemical compounds in the samples were determined by X-ray photoelectron spectroscopy with an ESCALAB MK II spectrometer (VG Scientific, the United Kingdom) equipped with a magnesium cathode as a source of nonmonochromatic MgK_α X-ray radiation (1253.6 eV). The spectra were processed using the C1s line (binding energy 284.6 eV) for calibration. The films were etched with an argon gun (Ar^+ ions) for 1 min at a mean rate of 0.1 nm s^{-1}.

The crystal structure and phase composition of the films were studied by X-ray diffraction with a Siemens D-5000 diffractometer using Cu$K_{\alpha1,2}$ radiation (λ = 1.54181 nm) in the angle interval 2θ = 10°–100° at 0.01° step with exposure 5 s in each point. The phase composition was analyzed using the Joint Committee on Powder Diffraction Standards (JCPDS) database.

The Raman spectra of thin films were taken with a Renishaw 1000 microscope-spectrometer using the green (514.5 nm) laser radiation. The laser power was 20 mW. The examined wavenumber range was from 200 to 1000 cm^{-1}. The integration time was 10 s.

RESULTS AND DISCUSSION

Based on the results of thermodynamic calculations [12], we prepared uniform tin(II) sulfide films on the glass–ceramic support with high adhesion to the support by hydrochemical deposition from tartrate and citrate–tartrate reaction mixtures using thioacetamide. The thickness of the synthesized layers varied from 100 to 650 nm depending on the synthesis conditions. The dependence of the SnS film thickness on the thioacetamide concentration for the process performed in the tartrate (curve *1*) and citrate–tartrate (curve *2*) systems is shown in Fig. 1. With an increase in the chalcogenizing agent concentration in the reaction bath, the layer thickness increases, and the film color gradually changes from golden to dark gray.

The use of a mixture of tartrate and citrate anions in the reaction bath allows smooth control of the layer thickness (Fig. 1) owing to the formation of tartrate and

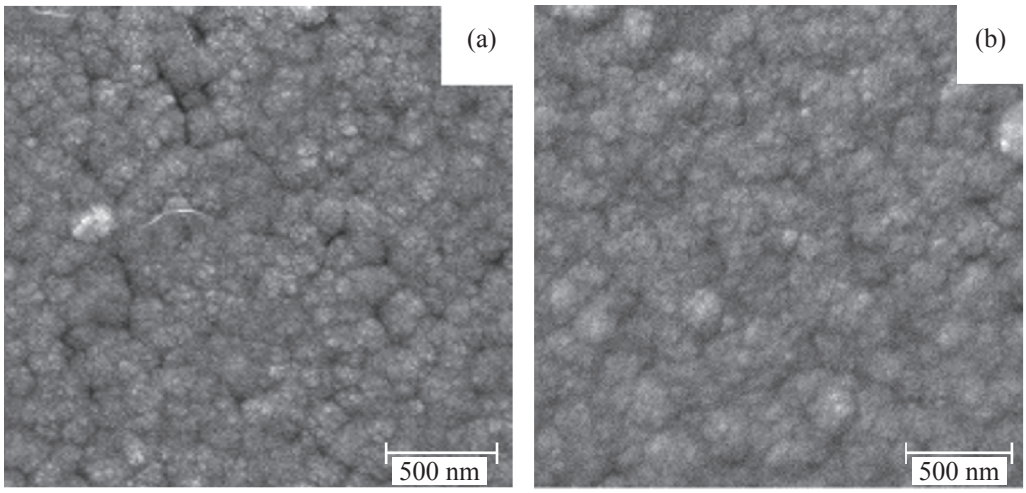

Fig. 2. SEM images of SnS films prepared from the citrate–tartrate reaction mixture at (a) 323 and (b) 333 K.

strong citrate complexes of tin. This mixture also allows the formation of chaotic surface landform of the films [3] to be avoided, which is critical for performing multilayer deposition. Therefore, our further studies were focused on deposition of tin sulfide with thioacetamide from the tartrate–citrate reaction mixture.

The surface relief of the tin(II) sulfide films prepared by hydrochemical deposition from the citrate–tartrate system was studied by scanning electron microscopy. Figure shows the electron-microscopic images of the surfaces of the freshly deposited SnS films synthesized at 323 (Fig. 2a) and 333 K (Fig. 2b). In both cases, the nanocrystalline character of the layers obtained is clearly pronounced. The synthesis at 323 K leads to the formation of spherical agglomerates approximately 200 nm in diameter, consisting of spherical nanocrystallites with a mean size of 20–40 nm, on the support surface. An increase in the deposition temperature in the citrate–tartrate system to 333 K does not appreciably influence the film morphology (Fig. 2b). In this case, the film thickness, according to the data of interference microscopy, decreased from 200 to 150 nm, and the size of nanocrystallites in globules increased to 50−60 nm.

We recorded the total X-ray photoelectron spectra of the samples in the range 0–1000 eV with a scanning step of 0.5 eV. To determine the chemical forms of elements in the surface layer of SnS, along with the total spectra we recorded the individual X-ray photoelectron spectra of the inner electron levels Sn3*d*, S2*p*, O1*s*, and C1*s*. The typical total spectra of the samples with the designated lines of the detected elements are shown in Fig. 3.

The data of X-ray photoelectron spectroscopy (XPS) show that the film samples obtained by hydrochemical deposition using thioacetamide as chalcogenizing agent are similar in composition and chemical bonds to tin(II) sulfide. The samples have strongly charged surface (up to 7.6 eV), which is caused both by the synthesis conditions and by the procedure of sample preparation for XPS analysis. The film etching with an argon beam cleans the sample surface to remove various contaminants, decreases the sample charging, and thus reduces the content of carbon and oxygen or virtually completely removes these elements.

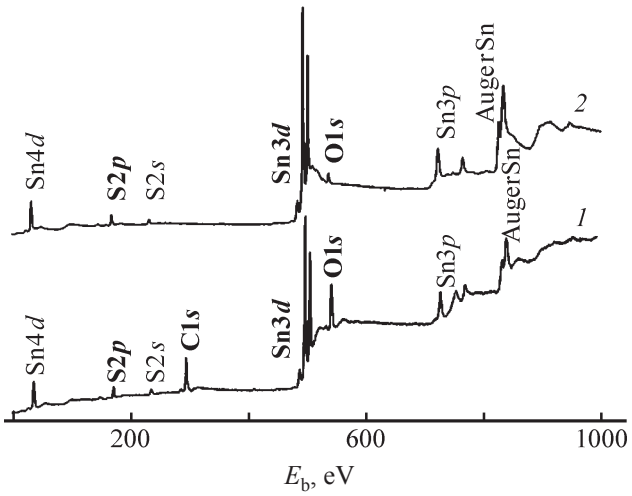

Fig. 3. Total XPS spectra of the surface of tin sulfide films deposited onto glass–ceramic (*1*) before etching and (*2*) after etching with an argon beam to a depth of 6 nm. (E_b) Binding energy; the same for Fig. 4.

Table 1. Content of the main forms of oxygen, tin, and sulfur in SnS films deposited from the citrate–tartrate system

SnS film	Content, at. % (electron level)								Charging, eV
	O1*s* (1)	O1*s* (2)	O1*s* (3)	Sn3*d* (1)	Sn3*d* (2)	Sn3*d* (3)	S2*p* (1)	Sn/S	
Surface	17.72	17.06	10.08	6.71	27.56	–	20.86	1.32	7.62
At a depth of 6 nm	11.90	1.80	–	3.64	45.78	8.73	28.18	1.62	6.65

Table 2. Energies of characteristic lines of elements in SnS films deposited from the citrate–tartrate system, taking into account charging

SnS film	Energy of characteristic lines, eV (electron level)							
	O1*s* (1)	O1*s* (2)	O1*s* (3)	Sn3*d* (1)	Sn3*d* (2)	Sn3*d* (3)	Sn4*d*	S2*p*
Surface	530.3	531.4	532.5	485.6	486.7		26.2	161.2
At a depth of 6 nm	530.3	533.5		484.7	486.1	486.8	25.3	161.3

Because of high content of carbon (~12 at. %) as component of surface contaminants, we calculated the content of sulfur, tin, and oxygen without taking into account carbon (Table 1).

The presence of oxygen in the layers follows from the presence of the O1*s* line in the spectrum. This line consists of several components (Table 2). The component with the higher binding energy (532.5−533.5 eV) can be assigned to C−O bonds in polyphenyl ether (vacuum oil of the diffusion pump) and to water molecules of hydration (the reference value of the O1*s* binding energy for water is from 533.1 to 538.0 eV), which is typical of surface contaminations [21]. The content of oxygen species giving these lines is up to 10.1 at. % (Table 1).

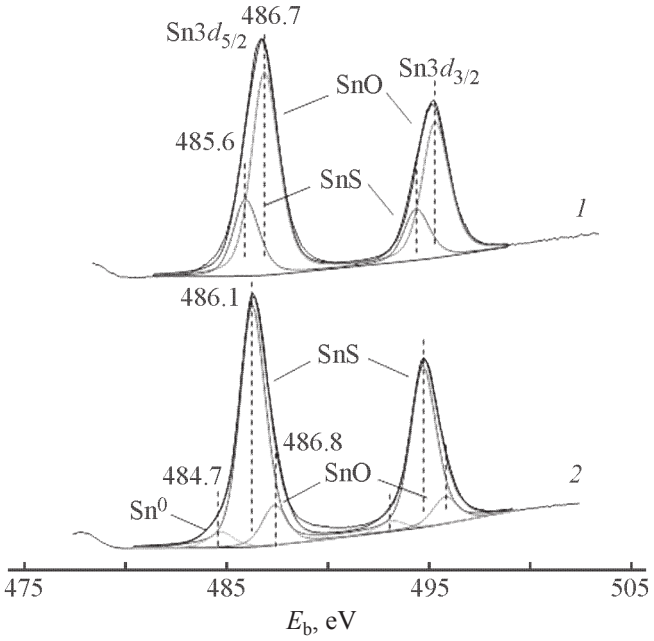

Fig. 4. Typical Sn3*d* XPS spectrum (splitting of Sn3$d_{3/2}$ and Sn3$d_{5/2}$ sublevels 8.42 eV) (*1*) before and (*2*) after etching of the tin sulfide film deposited with thioacetamide from the citrate–tartrate system.

The low-energy component (O1*s* binding energy 530.3 eV) can be assigned to tin monoxide SnO. According to data of Table 1, the content of oxide oxygen is 17.72 at. %. After 1-min etching with an argon beam, the content of oxygen incorporated in tin oxide decreased to 11.9 at %. The O1*s* line with the binding energy of 531.4 eV suggests the presence of carbonates and hydroxy groups OH^-, sorbed from the aqueous solution in the course of hydrochemical deposition, in the surface layers [22]. The content of oxygen incorporated in these species is up to 17.1 at. % (Table 1).

The Sn3*d* spectra of the films synthesized using thioacetamide (Fig. 4) show that tin exists in several states. The low-energy component (484.7 eV), which appears after the ion etching of the film and is associated with reduction of charged tin ions in the course of selective removal of lighter elements of the film, primarily of oxygen, can be assigned to elemental tin, Sn^0. The amount of elemental tin ranges from 4 to 5.5 at %.

The nonstoichiometric composition with respect to tin and sulfur, according to the EDX and XPS data, suggests the presence of X-ray amorphous tin hydroxides in the films [23]. This is confirmed by studies dealing with chemical deposition of tin sulfide [11, 13, 14]. It should be noted that the formation of concomitant impurity

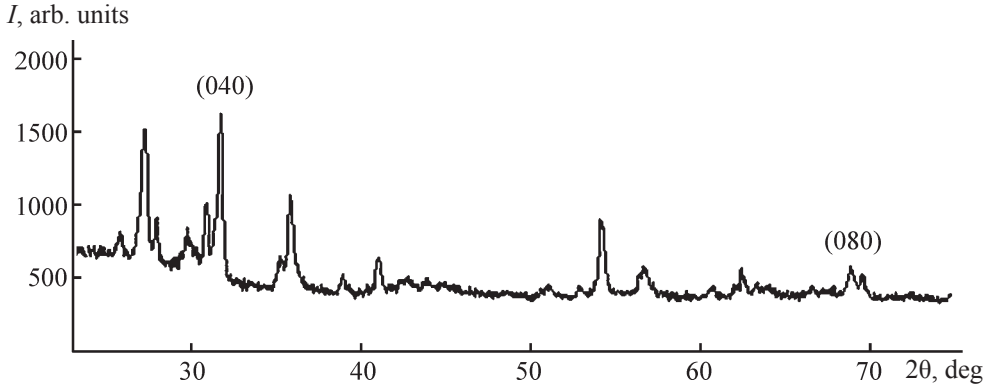

Fig. 5. X-ray diffraction pattern of the SnS film deposited onto glass–ceramic support from the citrate–tartrate reaction system. (*I*) Intensity and (2θ) Bragg angle.

phases will significantly influence the crystallization of tin sulfide films and, correspondingly, their properties.

The formation of tin sulfide SnS is confirmed by the component with the binding energy of 485.6−486.1 eV. The reference value for tin disulfide SnS_2 is 486.8 eV, which appreciably exceeds the value obtained. According to the calculations, the content of tin incorporated in the sulfide is from 27.6 (on the surface) to 45.8 at. % (at a depth of 6 nm) and in some cases exceeds the sulfur content by a factor of approximately 1.5. The revealed sulfur deficiency may be due to selective removal of elements in the course of argon beam etching.

According to the X-ray diffraction data, thin SnS films prepared by chemical deposition from the citrate–tartrate system crystallize in the orthorhombic system with the unit cell parameters a = 4.276, b = 11.243, and c = 3.986 Å (JCPDS 32-1361). These values are very close to the published data [24]. The reflections corresponding to the (040) and (080) reflections are noted in Fig. 5; the other reflections belong to the glass–ceramic support.

The formation of the tin(II) sulfide phase upon deposition from the citrate–tartrate system with thioacetamide is confirmed by the Raman data (Fig. 6). The major peak of the Raman spectrum, 222 cm^{-1}, characterizes the Sn–S bond. Its position virtually coincides with that reported by other authors: 218 [25] and 219 cm^{-1} [26].

CONCLUSIONS

(1) SnS films from 100 to 650 nm thick with good adhesion to a glass–ceramic support were prepared by hydrochemical deposition in the Sn^{2+}–$C_4H_6O_6$–$CSCH_3NH_2$ and Sn^{2+}–$C_4H_6O_6$–$Na_3C_6H_5O_7$–$CSCH_3NH_2$ systems in the temperature interval 323−343 K.

(2) The SnS films deposited from the citrate–tartrate reaction system have nanocrystalline character. Synthesis at 323 K leads to the formation of spherical agglomerates consisting of spherical nanocrystallites of 20–40 nm size on the support surface.

(3) According to the data of X-ray photoelectron spectroscopy, the surface layers of SnS films prepared from the citrate–tartrate system contain up to 14 at. % oxygen incorporated in oxygen-containing phases and surface contaminations. Their content sharply decreases with increasing depth. Tin in the synthesized layers, according to the XPS data, is in the bivalent state.

(4) X-ray diffraction analysis show that tin sulfide films

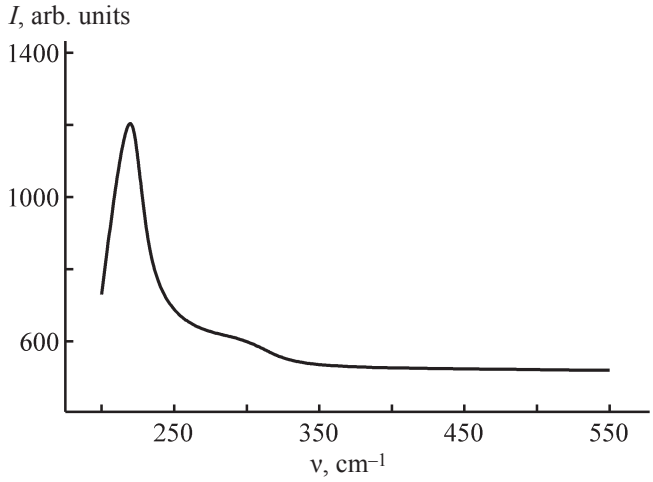

Fig. 6. Raman spectrum of the SnS film freshly deposited from the $SnCl_2$–Na_3Cit–$C_6H_6O_4$–$CSCH_3NH_2$ system. (*I*) Intensity and (ν) wavenumber.

crystallize in the orthorhombic system with the unit cell parameters $a = 4.276$, $b = 11.243$, and $c = 3.986$ Å.

REFERENCES

1. Bashkirov, S.A., Gremenok, V.F., Ivanov, V.A., and Shevtsova, V.V., *Phys. Solid State,* 2012, vol. 54, no. 12, pp. 2497–2502.
2. Devika, M., Reddy, N.K., Reddy, D.S., et al., *J. Phys.: Condens. Matter,* 2007, vol. 19, pp. 1–12.
3. Fedorova, E.A., Bazanova, E.A., Maskaeva, L.N., and Markov, V.F., *Chim. Tech. Acta*, 2014, vol. 1, no. 2, pp. 76–81.
4. Banai, R.E., Horn, M.W., and Brownson, J.R.S., *Solar Energy Mater. Solar Cells,* 2015, vol. 150, pp. 112–129.
5. Satheeshkumar, P.S. and Amalraj, L., *Chem. Pharm. Sci.,* 2015, pp. 52–54.
6. Sinsermsuksakul, P., Hartman, K., Kim, S.B., et al., *Appl. Phys. Lett*., 2013, vol. 102, pp. 053901–053905.
7. Jiang, T., Ozin, G.A., Verma, A., and Bedard, R.L., *J. Mater. Chem*., 1998, vol. 8, no. 7, pp. 1649–1656.
8. Sinsermsuksakul, P., Heo, J., Noh, W., et al., *Adv. Energy Mater.,* 2011, vol. 1, pp. 1116–1125.
9. Akkari, A., Guasch, C., and Kamoun-Turki, N., *J. Alloys Compd*., 2010, vol. 490, pp. 180–183.
10. Guneri, E., Gumus, C., Mansur, F., and Kirmizigul, F., *Optoelectron. Adv. Mater.—Rapid Commun*., 2009, vol. 3, no. 4, pp. 383–389.
11. Maskaeva, L.N., Fedorova, E.A., Shemyakina, A.I., et al., *Butlerovsk, Soobshch*., 2014, vol. 37, no. 2, pp. 1–9.
12. Maskaeva, L.N., Tulenin, S.S., Timina, A.A., et al., *Butlerovsk. Soobshch*., 2016, vol. 45, no. 3, pp. 72–79.
13. Markov, V.F., Maskaeva, L.N., Tret'yakova, N.A., and Epaneshnikova, D.S*., Fundam. Probl. Sovrem. Materialoved*., 2005, no. 2, pp. 59–60.
14. Chalapathi, U., Poornaprakash, B., and Park, S.-H., *J. Alloys Compd*., 2016, vol. 689, pp. 938−944.
15. Chalapathi, U., Poornaprakash, B., and Park, S.-H*., Solar Energy*, 2016, vol. 39, pp. 239−249.
16. Mukherjee, A. and Mitra, P*., Indian J. Phys*., 2015, vol. 89, pp. 1007−1012.
17. Jayasree, Y., Chalapathi, U., and Raja, V.S., *Thin Solid Films*, 2013, vol. 537, pp. 149–155.
18. Rana, T.R., Shinde, N.M., and Kim, J., *Mater. Lett*., 2016, vol. 162, pp. 40−43.
19. Du, M., Yin, X., and Gong, H., *Mater. Lett.,* 2015, vol. 152, pp. 40−44.
20. Gedi, S., Minnam Reddy, V.R., Pejjai, B., et al., *Appl. Surf. Sci*., 2016, vol. 372, pp. 116−124.
21. Patel, T.H., *Open Surf. Sci. J*., 2012, vol. 4, pp. 6–13.
22. Polivtseva, S., Oja Acik, I., Katerski, A., et al*., Energy Proc*., 2014, vol. 60, no. C, pp. 156–165.
23. Semenov, V.N., Ovechkina, N.M., and Khoviv, D.A., *Vestn. Voronezhsk. Gos. Univ., Ser. Khim., Biol., Farm*., 2007, no. 2, pp. 50–56.
24. Bashkirov, S.A., Gremenok, V.F., and Ivanov, V.A., *Semiconductors,* 2011, vol. 45, no. 6, pp. 749–752.
25. Raadik, T., Grossberg, M., Raudoja, J., and Krustok, J., *J. Phys. Chem. Solids*, 2013, vol. 74, pp. 1683–1685.
26. Sinsermsuksakul, P., Heo, J., Noh, W., et al., *Adv. Energy Mater*., 2011, vol. 1, pp. 1116–1125.